PERGAMON

International Journal of Solids and Structures 38 (2001) 3213–3232

INTERNATIONAL JOURNAL OF SOLIDS and STRUCTURES

www.elsevier.com/locate/ijsolstr

M-integral analysis for two-dimensional solids with strongly interacting microcracks. Part II: in the brittle phase of an infinite metal/ceramic bimaterial

Yi-Heng Chen *

Department of Engineering Mechanics, School of Civil Engineering and Mechanics, Xi'an Jiaotong University, Xi'an, Shaanxi 710049, People's Republic of China

Received 8 October 1999; in revised form 23 May 2000

Abstract

In order to extend the investigation addressed in Part I of this series to treat the multi-cracks problem in a finite brittle solid, this paper deals with the *M*-integral analysis for microcrack damage in the brittle phase of a metal/ceramic bimaterial. The basic idea is based on such a concept that the outside boundaries of the finite solid could be considered as a special kind of interface between air and the solid or between a rigid body and the solid. Following the work did by Zhao and Chen (Archive of Applied Mechanics 67, 393–406), who have found the contribution induced from the interface of the bimaterial to the J_2-integral, the first task of this paper is to reexamine the conservation laws of the J_k-vector in the interaction problem among the interface and multi-subinterface microcracks. Unlike the conclusion given in Part I, the vanishing nature of both components of the J_k-integral vector at infinity should include the contribution arising from the interface (as another kind of discontinuity). Only after clarifying this contribution, could new formulations of the conservation laws of the vector be deduced. This will lead to a correct way, from which the extension of the present investigation to treat a finite solid could be performed. Furthermore, the second task of this paper is aimed at providing a fundamental understanding of the interaction effect and the coalescence tendency for the microcracks based on the *M*-integral analysis as influenced by the existence of the ductile phase. Numerical results are given for the Cu/Al_2O_3 and the Ni/MgO bimaterial solids. It is concluded that the *M*-integral actually plays an important role for microcrack damage in the brittle phase of the bimaterial solids, which could be considered as a measure of the damage level and the coalescence tendency among the microcracks. It is concluded also that for a certain microcrack array the value of the *M*-integral in metal/ceramic bimaterial solids is always larger than that in homogeneous brittle solids. This means that the same microcrack array in the former cases shows lower stability and larger coalescence tendency than that in the later cases due to the existence of the ductile phase or due to the interaction of the microcrack array with the interface. Of great interest is that the divergencies of the *M*-integral values in bimaterials from those for the same microcrack array in homogeneous brittle solids are dominated by the first Dundurs parameter with no regards to the second Dundurs parameter. Finally, an extension of this investigation to treat microcrack damage in a half plane brittle solid is discussed briefly to show the potential applications of the *M*-integral analysis.

* Tel.: +86-29-2660404; fax: +86-29-323-7910.
E-mail addresses: yhchen2@xjtu.edu.cn, yhc22@eng.cam.ac.uk (Y.-H. Chen).

0020-7683/01/$ - see front matter
PII: S0020-7683(00)00243-2

Keywords: Bimaterial; Brittle phase; Interface; Subinterface cracks; Damage

1. Introduction

As well-known, path-independent integrals proposed in plane fracture mechanics could be divided into two catalogues. Some of them are concerned only with the computation of critical parameters associated with one single crack extension since they involve only the evaluation of path-independent contour integrals, the data for which are available from numerical solutions for boundary value problems under consideration without any special treatment of the near-tip region of the crack (see e.g., Freund, 1978; Stern et al., 1976; Chen, 1985). However, the others have some definite physical meanings. For example, besides the well-known *J*-integral (Rice, 1968) with a precise and clear physical significance as the rate of total potential energy release per unit crack-tip advance, the *L*-integral and the *M*-integral (Knowles and Sternberg, 1972; Budiansky and Rice, 1973) have been given as the crack rotational energy release rate and the crack uniform expansion energy release rate, respectively (Herrmann and Herrmann, 1981).

On the other hand, interface cracks including subinterface cracks in bimaterial solids in view of their importance in numerous applications have received considerable attention in the past twenty years (see e.g., Hutchinson et al., 1987; Park and Earmme, 1986; He and Hutchinson, 1989; Lardner et al., 1990; Evans et al., 1986; Chen and Lardner, 1993; Chen and Hasebe, 1994; Rice, 1988; Suo and Hutchinson, 1989; 1990; Suo, 1989; Lu and Lardner, 1992). Recently, the interaction of microcracks in the near-tip process zone with an interface crack and the interaction among multiple subinterface cracks are investigated (see, Isida and Noguchi, 1994; Zhao and Chen, 1996; 1997a,b). It is found that a conservation law does exist among three values of the *J*-integral respectively contributed by the macro-interface crack tip, the microcracks in the near-tip process zone, and the remote stress field. It is found also that the contribution to the *J*-integral arising from the existence of the microcracks could be evaluated by using the projected values of the J_k-vector defined in a local system for each microcrack (Zhao and Chen, 1997a). Moreover, it is concluded that for multi-subinterface cracks, the summation of the first component of the J_k-vector arising from all the cracks vanishes due to the zero contribution induced from the interface to the J_1-integral (Zhao and Chen, 1997b). However, the summation of the second component of the J_k-vector, generally speaking, does not vanish due to the non-zero contribution induced from the interface to the J_2-integral when the chosen integral contour cuts the interface and encloses a segment of the interface (Zhao and Chen, 1997b).

This paper has two goals. First, as a progress of the investigation addressed in Part I, the conservation laws of the J_k-vector and the independence of the *M*-integral from the selection of global coordinates for a cloud of interacting microcracks in the brittle phase of metal/ceramic bimaterial solids are reexamined. Special attention is focused on the contribution induced from the whole interface to the second component of the vector when setting the origin of coordinates not on the interface and taking an infinite large closed contour surrounding all the discontinuities completely. Only after doing so, could the restriction arising from the discussion in Part I of this series be removed. Second, a fundamental understanding of the interaction effect and the coalescence tendency for the subinterface microcracks is given by using the *M*-integral analysis in metal/ceramic bimaterials. Numerical results for Cu/Al_2O_3 and Ni/MgO bimaterial solids show that the *M*-integral does not actually depend on the selection of the global coordinates and it does play an important role for evaluating microcrack damage in the brittle phase of metal/ceramic bimaterial solids. It is concluded that the *M*-integral is divided into two distinct parts similar to those did in Part I of this series. However, the formulation of the second part called as the additional part is not only concerned with the contribution induced from the J_k-vector and the coordinates of each crack center, but also with the contribution induced from the whole interface (as another kind of discontinuity). Detailed manipulations reveal that the later contribution does not lead to the dependence of the integral on the

selection of the global coordinates, either on the movement or on the rotation of the global coordinates. Moreover, numerical results show that, in the most cases of microcrack configurations under consideration, the net-part of the integral could not always provide overwhelming superiority over the additional part of the integral. A number of comparisons between the results in bimaterial solids and those in homogeneous solids are performed. It is found that the values of the M-integral in the metal/ceramic solids are always larger than the corresponding values arising from the same microcrack configurations in homogeneous brittle solids. This means that a certain microcrack array in the brittle phase of metal/ceramic solids shows lower stability and larger coalescence tendency than the corresponding one in homogeneous brittle solids due to the existence of the ductile phase. Of great interest is that the divergencies of the M-integral values in metal/ceramic bimaterials from those for the same microcrack array in homogeneous brittle solids are dominated by the first Dundurs parameter with no regards to the second Dundurs parameter.

The extension of the present investigation to treat the multi-cracks problem in a half plane solid is discussed briefly by considering the outside boundaries of the solid as a special kind of interface between air and the solid. It is emphasized that this is the only correct way to study the conservation laws of the J_k-integral vector and the M-integral for microcrack damage in a finite brittle solid.

2. Conservation laws of the J_k-vector in bimaterials

The microcrack damage problem considered here is shown in Fig. 1, in which N microcracks are formed in the brittle phase (i.e., the material 2 occupies the lower half plane) of a metal/ceramic bimaterial solid. The microcracks may be induced from thermal mismatch, impact or other sources, which may have different lengths (denoted by $2a_k$) and different oriented angles with respect to the interface (denoted by ϕ_k).

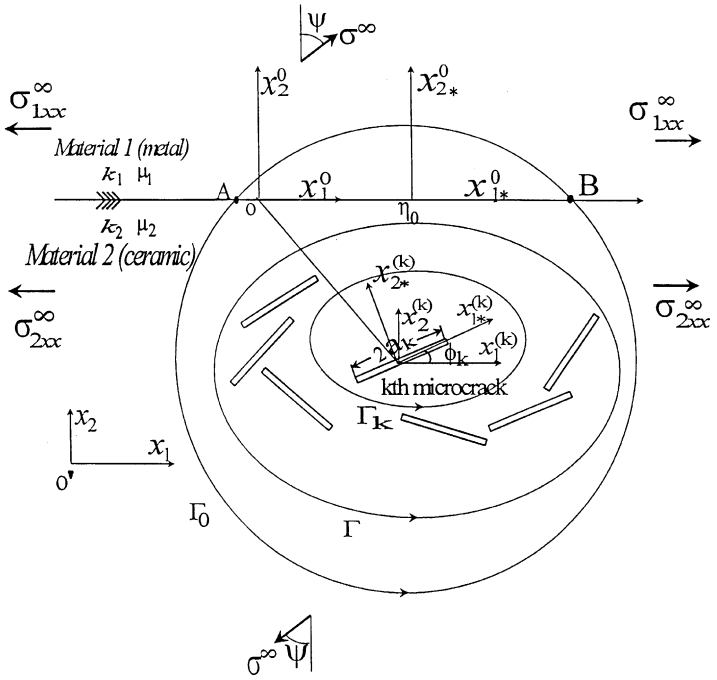

Fig. 1. A cloud of interacting microcracks beneath the interface in a metal/ceramic bimaterial solid.

Two global coordinate systems are introduced respectively, say, (x_1^0, x_2^0) and (x_1, x_2). The origin of (x_1^0, x_2^0) is taken to be located on the interface and the x_1^0-axis to be parallel to the interface, while the origin of (x_1, x_2) is taken to be not located on the interface and the x_1-axis to be still parallel to the interface (see Fig. 1). Therefore, the coordinates of microcrack centers in (x_1^0, x_2^0) denoted by $(\xi_1^{0(k)}, \xi_2^{0(k)})$ and those in (x_1, x_2) denoted by $(\xi_1^{(k)}, \xi_2^{(k)})$ are related by

$$\xi_1^{(k)} = \xi_1^{0(k)} + \eta_1, \qquad \xi_2^{(k)} = \xi_2^{0(k)} + \eta_2 \quad (k = 1, 2, \ldots, N), \tag{1}$$

where the superscript (k) refers to the kth microcrack, and η_1 and η_2 are constants which represent the translation from the system (x_1^0, x_2^0) to the system (x_1, x_2).

Besides these, two local coordinate systems are also introduced for a typical microcrack (k) below the interface. Here, $(x_1^{(k)}, x_2^{(k)})$ is parallel to (x_1^0, x_2^0), while $(x_{1^*}^{(k)}, x_{2^*}^{(k)})$ is oriented with respect to $(x_1^{(k)}, x_2^{(k)})$ by ϕ_k. Three kinds of closed contours, i.e., Γ_0, Γ and Γ_k are introduced (see Fig. 1). Here, Γ_0 encloses all the microcracks and cuts the interface at the points A and B, Γ encloses all the microcracks but does not cut the interface, and Γ_k encloses the kth microcrack only but does not cut the interface.

The bimaterial solid is loaded by the remote tensile stress σ^∞ with an inclined angle ψ and the remote horizontal stresses σ_{1xx}^∞ and σ_{2xx}^∞.

According to the path-independent nature of the J_k-integral vector, the following formulations are valid (Knowles and Sternberg, 1972; Budiansky and Rice, 1973):

$$J_k(\Gamma_0) = \int_{\Gamma_0} (Wn_k - T_l u_{l,k})\,\mathrm{d}s = J_k(\Gamma) + J_k(AB) \quad (k = 1, 2), \tag{2}$$

where $J_k(\Gamma_0), J_k(\Gamma)$, and $J_k(AB)$ denote the values of the vector calculated along the three different contours Γ_0, Γ, and AB, respectively (see Fig. 1). The last two ones could be given as follows:

$$J_k(\Gamma) = \sum_{K=1}^{N} J_k(\Gamma_K) \quad (k = 1, 2), \tag{3a}$$

$$J_k(AB) = \int_{AB} ([W]n_k - T_l[u_{l,k}])\,\mathrm{d}s \quad (k = 1, 2), \tag{3b}$$

where [ ] denotes the jump of the corresponding quantities across the interface.

Obviously,

$$J_1(\overline{AB}) = \int_{\overline{AB}} ([W]n_1 - T_l[u_{l,1}])\,\mathrm{d}s = 0 \tag{4}$$

due to the fact that the component n_1 vanishes and the displacement continuity conditions across the interface are met.

Therefore, the conservation law for the first component of the vector is still valid (see Eqs. (13a) and (13b) or (15) in Part I of this series). Attention should only be focused on the J_2-integral analysis in Eqs. (2) and (3b) to establish a new law instead of Eq. (14) or (15) in Part I.

According to the work did by Smelser and Gurtin (1977), the following equation is valid in a bimaterial without cracks:

$$J_2 = \int_{\Gamma_0} (Wn_2 - \sigma_{ij} n_j u_{i,2})\,\mathrm{d}s - \int_l ([w] - \sigma_{i2}[u_{i,2}])\,\mathrm{d}s = 0, \tag{5}$$

where Γ_0 refers to a closed contour cutting the interface at points A and B, while l refers to the segment of the interface from A to B.

For the multi-subinterface cracks shown in Fig. 1, it follows that:

$$\int_{\Gamma_0}(Wn_2-\sigma_{ij}n_ju_{i,2})\,\mathrm{d}s=\int_l([w]-\sigma_{i2}[u_{i,k}])\,\mathrm{d}s+\int_\Gamma(Wn_2-\sigma_{ij}n_ju_{i,2})\,\mathrm{d}s, \tag{6}$$

where Γ is a closed contour surrounding all the cracks but does not cut the interface (see Fig. 1).

Assume that the stress field and the displacement field consist of two distinct parts. One of them is induced from the uniform remote loading conditions and the other is induced from the existence of the subinterface multi-cracks

$$\sigma_{ij}=\sigma_{ij}^{\mathrm{U}}+\sigma_{ij}^{\mathrm{E}},\qquad u_i=u_i^{\mathrm{U}}+u_i^{\mathrm{E}}\quad(i,j=1,2), \tag{7}$$

where the superscripts U and E refer to the uniform remote loading and the existence of the cracks, respectively.

Thus, Eq. (6) could be reformulated as

$$\begin{aligned}&\int_{\Gamma_0}((W^{\mathrm{U}}+W^{\mathrm{E}}+W^{\mathrm{UE}}+W^{\mathrm{EU}})n_2-(\sigma_{ij}^{\mathrm{U}}+\sigma_{ij}^{\mathrm{E}})n_j(u_{i,2}^{\mathrm{U}}+u_{i,2}^{\mathrm{E}}))\,\mathrm{d}s\\&\quad=\int_l([W^{\mathrm{U}}+W^{\mathrm{E}}+W^{\mathrm{UE}}+W^{\mathrm{EU}}]n_2-(\sigma_{ij}^{\mathrm{U}}+\sigma_{ij}^{\mathrm{E}})n_j[u_{i,2}^{\mathrm{U}}+u_{i,2}^{\mathrm{E}}])\,\mathrm{d}s+\int_\Gamma((W^{\mathrm{U}}+W^{\mathrm{E}}+W^{\mathrm{UE}}+W^{\mathrm{EU}})n_2\\&\qquad-(\sigma_{ij}^{\mathrm{U}}+\sigma_{ij}^{\mathrm{E}})n_j(u_{i,2}^{\mathrm{U}}+u_{i,2}^{\mathrm{E}}))\,\mathrm{d}s,\end{aligned} \tag{8}$$

where the superscript UE and EU refer to the interleaving terms contributed by the stresses arising from the remote loading and the displacements arising from the existence of the cracks or vice versa.

Obviously, the summation among the interleaving terms vanishes due to the well-known Betii-reciprocal theory. Therefore, Eq. (8) leads to

$$\begin{aligned}\int_{\Gamma_0}((W^{\mathrm{U}}+W^{\mathrm{E}})n_2-(\sigma_{ij}^{\mathrm{U}}n_ju_{i,2}^{\mathrm{U}}+\sigma_{ij}^{\mathrm{E}}n_ju_{i,2}^{\mathrm{E}}))\,\mathrm{d}s&=\int_l([W^{\mathrm{U}}+\dot{W}^{\mathrm{E}}]n_2-(\sigma_{ij}^{\mathrm{U}}n_j[u_{i,2}^{\mathrm{U}}]+\sigma_{ij}^{\mathrm{E}}n_j[u_{i,2}^{\mathrm{E}}]))\,\mathrm{d}s\\&\quad+\int_\Gamma((W^{\mathrm{U}}+W^{\mathrm{E}})n_2-(\sigma_{ij}^{\mathrm{U}}+\sigma_{ij}^{\mathrm{E}})n_j(u_{i,k}^{\mathrm{U}}+u_{i,2}^{\mathrm{E}}))\,\mathrm{d}s.\end{aligned} \tag{9}$$

When setting the closed contour Γ_0 to be infinite large so that the whole interface from $-\infty$ to ∞ is enclosed in it, the physical quantities σ_{ij}^{E}, u_i^{E}, W^{E} on Γ_0 vanish due to they asymptote nature at infinity. But they may not vanish on the closed contour Γ or on the interface from $-\infty$ to ∞. By substituting Eq. (5) into (9), the latter becomes

$$\int_{-\infty}^{\infty}([W^{\mathrm{E}}]n_2-\sigma_{ij}^{\mathrm{E}}n_j[u_{i,2}^{\mathrm{E}}])\,\mathrm{d}s+\int_\Gamma(W^{\mathrm{E}}n_2-\sigma_{ij}^{\mathrm{E}}n_ju_{i,2}^{\mathrm{E}})\,\mathrm{d}s=0 \tag{10}$$

which could simply be reformulated as

$$\sum_{k=1}^{N}J_2^{(k)}+J_{2\infty}=0 \tag{11}$$

keeping in mind that the two terms in the left side of Eq. (11) denote the contributions of the N subinterface cracks and the whole interface to the J_2-integral, respectively.

In other words, the contribution induced from the subinterface multi-cracks cancels with those induced from the whole interface. Therefore, Eq. (11) does represent a new conservation law in bimaterials, which will be found to be very useful in the forthcoming manipulations about the M-integral analysis.

As regards the numerical methods, obviously, the first term in Eq. (11) is the summation of the contributions induced from each subinterface crack. It could be calculated by using Eqs. (7), (8) and (10) in

Part I of this series when the interaction problem shown in Fig. 1 is solved (Zhao and Chen, 1997b). Of course, the local-global coordinate translation should be adopted (see Fig. 1) and the contribution induced from the traction-free surfaces of each crack should be taken into account (Herrmann and Hermann, 1981). However, the second term in Eq. (11) provides a new problem, which should be solved by developing a new technique for treating the infinite integral intervals involved. Such a technique is similar to that cited in Appendix B of Part I by using the Chebyshev Polynomial and the Chebyshev integration together with some variable translation (Hutchinson et al., 1987). This topic is no longer repeated here for shortening the length of this paper.

In order to confirm the new conservation law (11), a numerical example is presented here. Without loss of generalities, a single subinterface crack is considered, which is parallel to the interface in the brittle phase of a bimaterial solid. The distance between the crack and the interface is denoted by h, while a refers to the half-length of the crack. The mathematical technique for solving the simple problem is based on the work did by Zhao and Chen (1997b), from which all the stress-displacement values at any point in the metal/ceramic bimaterial could then be given without any difficulty. Thus, the contributions of the subinterface crack and the whole interface $(-\infty, +\infty)$ to the J_2-integral could be calculated numerically. Numerical results for Cu/Al_2O_3 bimaterial solid and under the remote loading $\sigma_{yy}^{\infty} = \sigma_{x2}^{\infty} = \sigma_{\infty} =$ constant are shown below

$$J_2 = \int_{-\infty}^{+\infty} ([W] - \sigma_{k2}[u_{k,2}])\,\mathrm{d}x = -0.1387576\frac{\sigma_{\infty}^2(1-\nu_2)\pi a^2}{2\mu_2} \tag{12a}$$

for the whole interface, and

$$J_2 = \int_{-a}^{a} ([W])\,\mathrm{d}x = 0.1387576\frac{\sigma_{\infty}^2(1-\nu_2)\pi a^2}{2\mu_2} \tag{12b}$$

for the subinterface crack, where [ ] denotes the jump of the corresponding quantities across the interface or across the subinterface crack.

Eqs. (12a) and (12b) are well agree with each other. They do confirm the new conservation law (11) for the J_2-integral. In other words, the total contribution of the subinterface crack and the whole interface to the J_2-integral vanishes, providing that the closed contour is taken to be infinite large, which encloses the whole interface as well as the crack. Indeed, this supports such a concept that the whole interface does represent a different kind of discontinuity from cracks.

In fact, by comparing Eq. (14) in Part I of this series with Eq. (11) in this paper, it is seen that the later could be considered as a special case of the former. If one uses N to denote the number of all the discontinuities in the bimaterial rather than the number of the cracks only, the former will become universal. Of course, other discontinuities, such as voids, kinking cracks, curve cracks or inclusions, can not alter the conservation laws of the J_k-vector if the closed contour encloses all kinds of discontinuities completely.

It should be emphasized also that the conservation laws of Eq. (11) mentioned above and Eqs. (13a) and (13b) in Part I are only suitable to treat the case with the interface perpendicular to the x_2-axis. If it is not so, for example, the interface is perpendicular to the x_1-axis rather than the x_2-axis, the above manipulations should be repeated for evaluating the J_1-integral rather than the J_2-integral. The laws should then be replaced by

$$\sum_{k=1}^{N} J_1^{(k)} + J_{1\infty} = 0, \tag{13a}$$

$$\sum_{k=1}^{N} J_2^{(k)} = 0, \tag{13b}$$

keeping in mind that $J_{1\infty}$ refers to the contribution induced from the whole interface to the first component of the vector.

3. Independence of the *M*-integral from the coordinate selection in bimaterials

After clarifying the role the J_k-vector plays in bimaterials with multi-subinterface cracks, the independence of the *M*-integral from the coordinate selection shown in Fig. 1 could be reexamined. In this section, analytical treatments are divided into two catalogues. First of them is associated with the global coordinates originated on the interface, while the second with the global coordinates not originated on the interface.

Special attention is always focused on the contribution arising from the segment *AB*. Indeed, confusion, if exists, is always induced from the misunderstanding or oversight of the segment. Up to date, it is not clear what happens to the *M*-integral in the present problem shown in Fig. 1 when choosing the different closed contours Γ (below the interface) or Γ_0 (across the interface), respectively. In fact, many people believe that the value of the *M*-integral should depend on the location of the coordinates. This confusion will be clarified below.

3.1. The origin of the coordinate system located on the interface

The global coordinate system (x_1^0, x_2^0) is assumed as originated on the interface (see Fig. 1). From the original definition of the *M*-integral as cited by Eq. (1) in Part I (Knowles and Sternberg, 1972; Budiansky and Rice, 1973), the *M*-integral calculated along Γ_0 in Fig. 1 should be equal to the summation of the contributions induced from the segment *AB* and Γ, respectively

$$M_{\Gamma_0}(x_1^0, x_2^0) = M_{AB}(x_1^0, x_2^0) + M_{\Gamma}(x_1^0, x_2^0), \tag{14}$$

where the subscripts Γ_0, *AB*, and Γ refer to the contributions calculated over the three contours, respectively (see Fig. 1). Since the origin of the system (x_1^0, x_2^0) lies on the interface (Park and Earmme, 1986), the first term in the right side is deduced to

$$M_{AB} = \int_{AB} ([W]x_i^0 n_i - T_i[u_{i,l}]x_l^0)\,\mathrm{d}s \quad (l, i = 1, 2). \tag{15}$$

Obviously, it vanishes in the present case due to the fact that $x_2^0 \equiv 0$, $n_1 \equiv 0$, and $[u_{i,1}] \equiv 0$. Therefore, the following manipulation could be given by making the translation from the global system (x_1^0, x_2^0) to the local system $(x_1^{(k)}, x_2^{(k)})$, i.e., Eq. (1)

$$\begin{aligned} M_{\Gamma_0}(x_1^0, x_2^0) = M_{\Gamma}(x_1^0, x_2^0) &= \sum_{k=1}^{N} M_{\Gamma_k}(x_1^0, x_2^0) = \sum_{k=1}^{N} \left\{ \int_{\Gamma_k} (W x_i^0 n_i - T_l u_{l,i} x_i^0)\,\mathrm{d}s \right\} \\ &= \sum_{k=1}^{N} \left\{ \int_{\Gamma_k} \left[W(x_i^{(k)} + \xi_i^{0(k)}) n_i - T_l u_{l,i}(x_i^{(k)} + \xi_i^{0(k)}) \right] \mathrm{d}s \right\} \\ &= \sum_{k=1}^{N} \left\{ \oint_{\Gamma_k} \left[W x_i^{(k)} n_i - T_l u_{l,i} x_i^{(k)} \right] \mathrm{d}s + \xi_i^{0(k)} \oint_{\Gamma_k} (W n_i - T_l u_{l,i})\,\mathrm{d}s \right\} \\ &= \sum_{k=1}^{N} \left\{ M_{\Gamma_k}(x_1^{(k)}, x_2^{(k)}) + \xi_1^{0(k)} J_1^{(k)} + \xi_2^{0(k)} J_2^{(k)} \right\}, \end{aligned} \tag{16}$$

where $M_{\Gamma_k}(x_1^{(k)}, x_2^{(k)})$ is evaluated along Γ_k in the local system $(x_1^{(k)}, x_2^{(k)})$, $J_1^{(k)}$ and $J_2^{(k)}$ are contributed by the kth microcrack, which could be evaluated by using the projected relations (see Eq. (7) in Part I or see Zhao and Chen, 1997a,b), which are cited here for convenience

$$J_1^{(k)} = J_{1^*}^{(k)} \cos\phi_k - J_{2^*}^{(k)} \sin\phi_k \qquad J_2^{(k)} = J_{1^*}^{(k)} \sin\phi_k + J_{2^*}^{(k)} \cos\phi_k \tag{17a}$$

and

$$\begin{aligned} J_{1^*}^{(k)} &= \frac{\kappa_2 + 1}{8\mu_2} \left[(K_{\mathrm{IR}}^{(k)})^2 + (K_{\mathrm{IIR}}^{(k)})^2 - (K_{\mathrm{IL}}^{(k)})^2 - (K_{\mathrm{IIL}}^{(k)})^2 \right] \\ J_{2^*}^{(k)} &= \frac{\kappa_2 + 1}{4\mu_2} \left[K_{\mathrm{IL}}^{(k)} K_{\mathrm{IIL}}^{(k)} - K_{\mathrm{IR}}^{(k)} K_{\mathrm{IIR}}^{(k)} \right] + F_{2^*}^{(k)}, \end{aligned} \tag{17b}$$

where the subscript star refers to the quantities in the local system $(x_{1^*}^{(k)}, x_{2^*}^{(k)})$ (see Fig. 1), the subscripts R and L denote the right and left tips of the kth microcrack, the subscripts I and II denote the Mode I and Mode II stress intensity factors, respectively, κ_2 and μ_2 are elastic constants of the brittle phase, i.e., the material 2, and $F_{2^*}^{(k)}$ denotes the contribution induced from the traction-free faces of the kth microcrack to the second component of the J_k-vector (Herrmann and Herrmann, 1981).

It is seen from Eq. (16) that the formulation of the M-integral in the present case is similar to Eq. (17e) in Part I for homogeneous brittle solids. It could also be divided into two distinct parts. One of them, i.e., the net-part denoted by M_N, is contributed by the crack tip stress intensity factors of each subinterface crack:

$$M_N = \sum_{k=1}^{N} M_{\Gamma_k}(x_1^{(k)}, x_2^{(k)}) = \sum_{k=1}^{N} \frac{\kappa_2 + 1}{8\mu_2} \left\{ (K_{\mathrm{IR}}^{(k)})^2 + (K_{\mathrm{IIR}}^{(k)})^2 + (K_{\mathrm{IL}}^{(k)})^2 + (K_{\mathrm{IIL}}^{(k)})^2 \right\} a_k, \tag{18}$$

where a_k refers to the half length of the kth microcrack. The other part, i.e., the additional part denoted by M_A, is induced from the coordinates of the kth microcrack center and the J_k-vector evaluated in the local system $(x_{1^*}^{(k)}, x_{2^*}^{(k)})$ and along the closed contour Γ_k

$$M_A = \sum_{k=1}^{N} \left\{ \xi_1^{0(k)} J_1^{(k)} + \xi_2^{0(k)} J_2^{(k)} \right\} \tag{19}$$

or in the local system $(x_{1^*}^{(k)}, x_{2^*}^{(k)})$

$$M_A = \sum_{k=1}^{N} \left\{ \xi_1^{0(k)} (J_{1^*}^{(k)} \cos\phi_k - J_{2^*}^{(k)} \sin\phi_k) + \xi_2^{0(k)} (J_{1^*}^{(k)} \sin\phi_k + J_{2^*}^{(k)} \cos\phi_k) \right\}. \tag{20}$$

However, it should be emphasized that all the physical quantities in Eqs. (17a)–(20) have been influenced by the existence of the interface. In other words, the values of the J_k-vector and the M-integral are quite different from those in homogeneous cases due to the interaction between the interface and the subinterface cracks. A fundamental understanding of the influence will be discussed in the next section.

Since the origin of the system (x_1^0, x_2^0) lies on the interface, the crack center coordinate $\xi_2^{0(k)} (k = 1, 2, \ldots, N)$ could not vary when the origin moves a distance, say η_0, from one point to other point on the interface (see Fig. 1). After the translation with the distance η_0 the formulation (19) becomes

$$M_A^* = \sum_{k=1}^{N} \left\{ \xi_1^{0(k)} J_1^{(k)} + \xi_2^{0(k)} J_2^{(k)} \right\} + \eta_0 \sum_{k=1}^{N} J_1^{(k)}, \tag{21}$$

where the superscript star $*$ denotes the quantities in a new system $(x_{1^*}^0, x_{2^*}^0)$ whose origin also lies on the interface, but whose vertical axis translates the distance η_0 (see Fig. 1).

As discussed above, the last term in the right side of Eq. (21) vanishes. Therefore, the independence of the M-integral from the global system selection has been proved since the interface segment AB has no contribution to the J_1-integral and in turn no contribution to the additional part of the M-integral

$$M_A = M_A^* \qquad M_N = M_N^*. \tag{22}$$

3.2. The origin of the coordinate system not located on the interface

Reconsider the microcrack damage problem shown in Fig. 1 but take another coordinate system (x_1, x_2), whose origin is not located on the interface. After performing some manipulations, the following formulation is given:

$$M_{\Gamma_0}(x_1,x_2) = M_{AB}(x_1,x_2) + M_{\Gamma}(x_1,x_2) = \sum_{k=1}^{N}\left\{M_{\Gamma_k}(x_1^{(k)},x_2^{(k)}) + \xi_1^{(k)}J_1^{(k)} + \xi_2^{(k)}J_2^{(k)}\right\} + M_{AB}(x_1,x_2), \tag{23}$$

where the last term $M_{AB}(x_1,x_2)$ is induced from the segment AB which should be specially considered with caution in the (x_1,x_2) system

$$M_{AB}(x_1,x_2) = \int_A^B (Wx_i n_i - T_l u_{l,i} x_i)\,\mathrm{d}s = \eta_2 \int_{x_{1A}}^{x_{1B}} \left[(W^+ - W^-) - (\sigma_{l2}^+ u_{l,2}^+ - \sigma_{l2}^- u_{l,2}^-)\right]\mathrm{d}x \tag{24}$$

in which η_2 is the vertical distance from the origin O' of (x_1,x_2) to the interface, x_{1A} and x_{1B} are the horizontal coordinates of points A and B on the interface (see Fig. 1), respectively, and the superscripts $+$ and $-$ refer to the upper boundary values and the lower boundary values on the interface, respectively.

Obviously, the path-dependency of the M-integral could be seen in Eq. (24) since different segment AB will lead to different value of $M_{AB}(x_1,x_2)$. However, when setting the closed contour Γ_0 to be infinite large so that the whole interface is enclosed, Eqs. (23) and (24) will then become

$$M_{\Gamma_\infty}(x_1,x_2) = \sum_{k=1}^{N}\left\{M_{\Gamma_k}(x_1^{(k)},x_2^{(k)}) + \xi_1^{(k)}J_1^{(k)} + \xi_2^{(k)}J_2^{(k)}\right\} + M_\infty(\eta_2) \tag{25}$$

and

$$M_\infty(\eta_2) = \eta_2 J_{2\infty} = \eta_2 \int_{-\infty}^{\infty} \left[(W^+ - W^-) - (\sigma_{l2}^+ u_{l,2}^+ - \sigma_{l2}^- u_{l,2}^-)\right]\mathrm{d}x, \tag{26}$$

where Eq. (26) could be evaluated after the interaction problem shown in Fig. 1 is solved (Zhao and Chen 1997b). Obviously, the value of $J_{2\infty}$ does not depend on the selection of the coordinates although the value of $M_\infty(\eta_2)$ may depend on η_2.

It should be emphasized that Eq. (11) has shown the vanishing nature of the total contribution arising from all the microcracks and the whole interface to the J_2-integral. When making a coordinate transformation from the (x_1,x_2) system to the (x_1^0,x_2^0) system whose origin lies on the interface, Eq. (25) yields that

$$\begin{aligned} M_{\Gamma_\infty}(x_1,x_2) &= \sum_{k=1}^{N}\left\{M_{\Gamma_k}(x_1^{(k)},x_2^{(k)}) + (\xi_1^{0(k)} + \eta_1)J_1^{(k)} + (\xi_2^{0(k)} + \eta_2)J_2^{(k)}\right\} + \eta_2 J_{2\infty} \\ &= \sum_{k=1}^{N}\left\{M_{\Gamma_k}(x_1^{(k)},x_2^{(k)}) + \xi_1^{0(k)}J_1^{(k)} + \xi_2^{0(k)}J_2^{(k)}\right\} + \eta_1\sum_{k=1}^{N}J_1^{(k)} + \eta_2\left(\sum_{k=1}^{N}J_2^{(k)} + J_{2\infty}\right). \end{aligned} \tag{27}$$

Obviously, the second term in the right side of Eq. (27) vanishes due to the validity of Eqs. (13a) and (13b) in Part I (the interface is parallel to the x_1-axis). The third term vanishes too due to the new

conservation law of the J_k-vector (11) established above, and therefore, Eq. (27) directly leads to the following conclusion:

$$M_{\Gamma_\infty}(x_1, x_2) = M_{\Gamma_0}(x_1^0, x_2^0) \tag{28}$$

which confirms the independence of the M-integral from the selection of the origin of the global coordinate system, whatever the origin lies on the interface or not.

It should be emphasized that Eq. (28) is conditional, i.e., the closed contour should be infinite large so that the whole interface is enclosed in it otherwise the finite segment AB on the interface leads to the path-dependency of the $M_{\Gamma_\infty}(x_1, x_2)$ integral. In the forthcoming manipulations, it is always assumed that the origin of the global coordinate system lie on the interface and the closed contour be infinite large.

As regards the rotation of the coordinates, it is easy to prove directly from the definition of the M-integral that its value remains unaltered when the rotation of the coordinate system occurs (see Appendix A in Part I or see Park and Earmme, 1986). Indeed, the value of the M-integral in bimaterials does not depend on the selection of the coordinates, either on the translation or on the rotation. The assumption is that the closed contour chosen beforehand has been chosen as infinite large and not only all the microcracks, but also the whole interface are enclosed in it. Therefore, the confusion mentioned above which has been bothering many people for a long time is clarified.

4. M-integral analysis for microcrack damage in the brittle phase

Numerical results of the M-integral analysis are given in this section for multi-microcracks beneath the interface in the brittle phase of metal/ceramic bimaterial solids. Here, the global coordinate system is always originated from a certain point on the interface so that the contribution of the microcracks to the M-integral could be evaluated by Eqs. (18) and (19) with no regards to those induced from the interface. The numerical results for crack tip SIF's as well as those contributed by the traction-free faces of the microcracks to the J_2-integral are computed by using the technique proposed by Zhao and Chen (1997b). The detailed derivation procedure is no longer repeated here. The bimaterial solids considered below are loaded by the remote tensile stress σ^∞ parallel to the vertical axis x_2^0. Moreover, two tensile stresses σ_{1xx}^∞ and σ_{2xx}^∞ are aided such that the following relation is met (Isida and Noguchi, 1994):

$$\sigma_{2xx}^\infty + \sigma^\infty \sin^2\psi = \frac{1}{1+\kappa_2}\left\{\frac{\mu_1}{\mu_2}(1+\kappa_2)(\sigma_{1xx}^\infty + \sigma^\infty \sin^2\psi) + \left[3 - \kappa_2 - \frac{\mu_2}{\mu_1}(3-\kappa_1)\right]\sigma_{yy}^\infty\right\}, \tag{29}$$

where

$$\sigma_{yy}^\infty = \sigma_{1yy}^\infty = \sigma_{2yy}^\infty = \sigma^\infty \cos^2\psi \tag{30}$$

and μ_1 and κ_1 are material constants of the upper material (see Fig. 1).

In the numerical results presented below, the stress σ_{2xx}^∞ is always assumed to be zone, while the stress σ_{1xx}^∞ does not appear in the manipulations and the calculations although Eq. (30) is actually met (Zhao and Chen,1997b).

4.1. Two microcracks

Four kinds of two microcrack configurations are considered as shown in Fig. 2(a)–(d), respectively. Here, d denotes the distance between the two centers of the microcracks, h denotes the distance from the center of one microcrack to the interface, and α_0 and ϕ_0 denote the location angle and the oriented angle, respectively. The lengths of the two microcracks are assumed to be equal with each other and all numerical

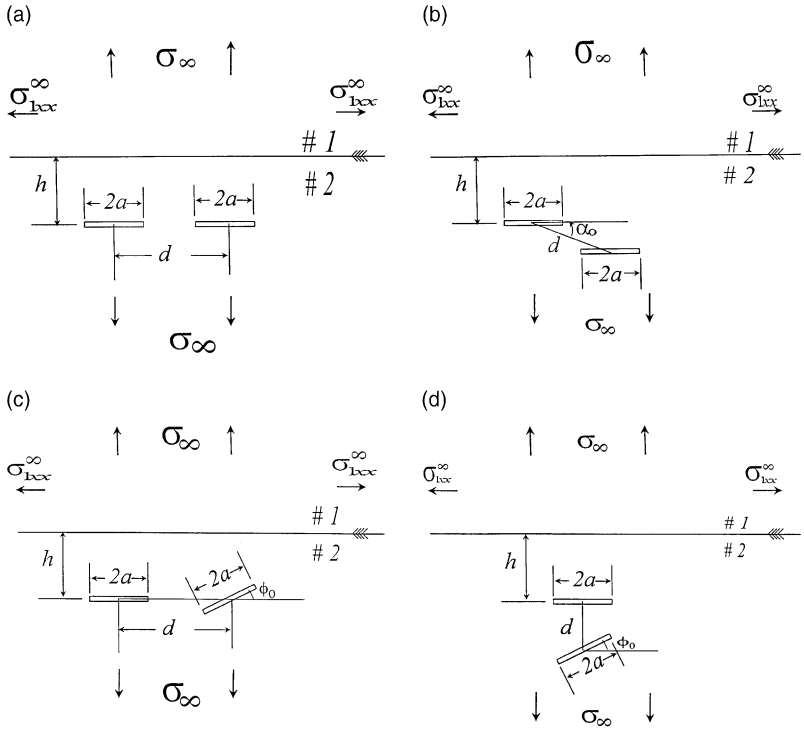

Fig. 2. (a)–(d) Four kinds of two-microcrack configuration.

Table 1
Dundurs' parameters and the oscillation index

Parameters	α	β	ε
Cu/Al_2O_3	−0.5118	−0.089	0.028
Ni/MgO	−0.138	0.015	−0.0049
Homogeneous	0.00	0.00	0.00
Air/Al_2O_3	−1	−1	Infinite

results are confirmed by the consistency check (13) of Part I (see Zhao and Chen, 1997b). Here Cu/Al_2O_3 and Ni/MgO bimaterial solids as well as a homogeneous elastic solid are considered for making comparisons. The ductile phase, i.e., Cu or Ni, always occupies the upper half plane, while the brittle phase, i.e., Al_2O_3 or MgO, always occupies the lower half plane. The Dundurs parameters α, β, and the oscillatory index ε for the two bimaterial solids are shown in Table 1 (Hutchinson et al., 1987). It is noted that α is always negative, while β is positive for Ni/MgO and negative for $CuAl_2O_3$, and ε is negative for Ni/MgO and positive for Cu/A_2O_3. Obviously, α, β, and ε are equal to zero in homogeneous cases.

All the computed values of the M-integral for the four configurations are normalized by

$$M_0 = \frac{\sigma_\infty^2 \pi (1 - \nu_2) a^2}{2\mu_2}, \tag{31}$$

where a refers to the half length of each microcrack and σ_∞ is the remote tensile stress which is always loaded along the direction perpendicular to the interface.

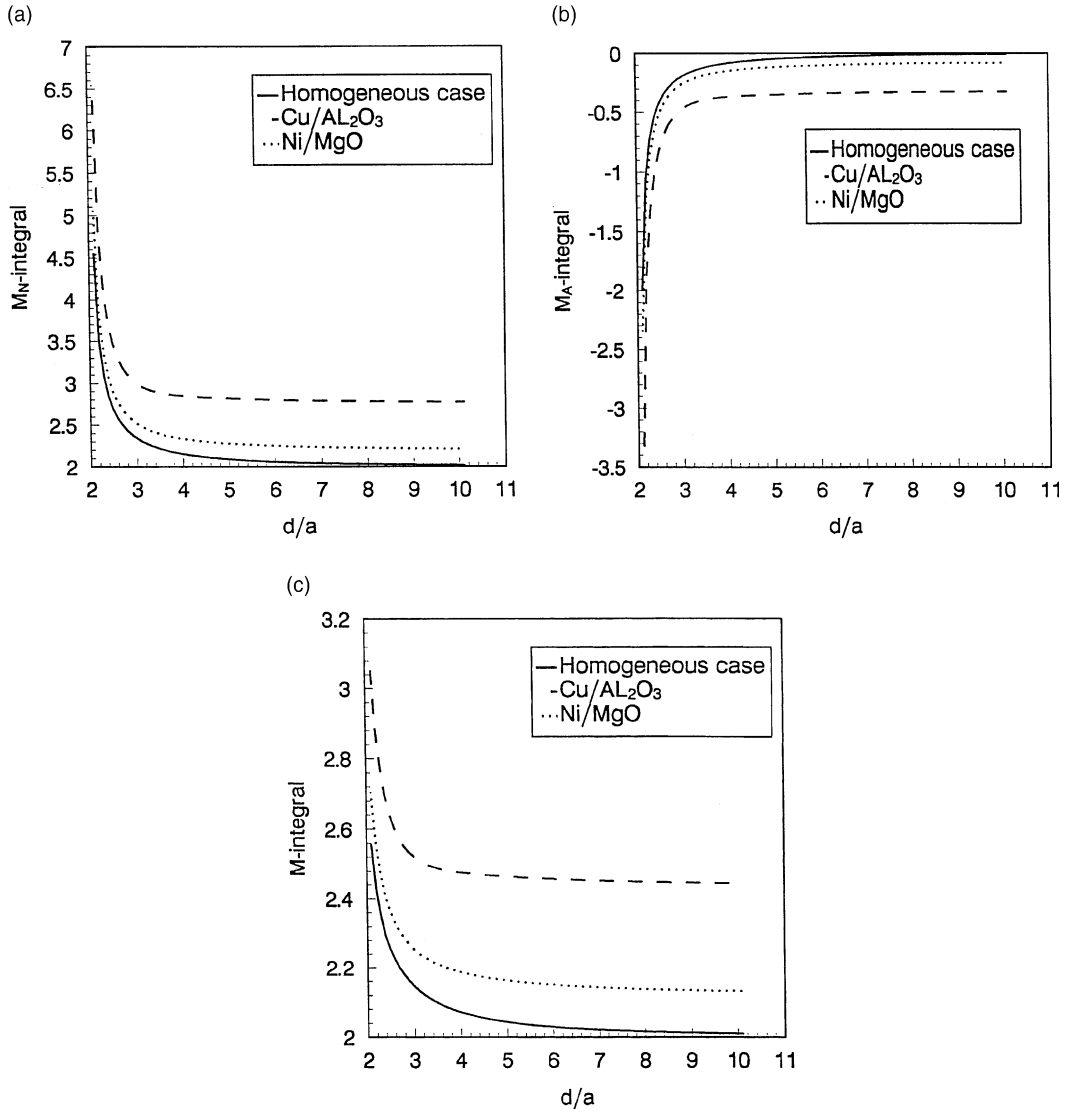

Fig. 3. (a)–(c) M_N, M_A, and M against d/a for the case of Fig. 2(a).

Nevertheless, the subinterface cracks are assumed to be stationary or no crack is allowed to grow. This could be ensured by controlling the remote tensile loading σ^{∞} together with Eq. (21b) in Part I. Computed values of M_N, M_A and M against the normalized distance d/a with $h/a = 1.25$ for the Fig. 2(a) are plotted in Fig. 3(a)–(c), respectively. All the values are normalized by Eq. (31) for making comparisons. The real curves refer to the results in homogeneous solids, the imaginary curves refer to the results in Cu/Al_2O_3 bimaterial solids, while the dotted curves refer to the results in Ni/MgO bimaterial solids. It is seen that, when d/a decreases for the collinear microcracks beneath the interface, the net part of the M-integral, M_N, always increases and the additional part of the M-integral, M_A, always decreases, while their summation, $M = M_N + M_A$, always increases, no matter what kind of metal/ceramic bimaterial solids is considered. This

means that in the present microcrack arrangement the M-integral is mainly governed by the net-part. Particularly, when $d/a > 4$, M_A is within ten percent of M and it could be neglected indeed. However, when $d/a < 4$, specially when $d/a < 3$, the contribution of M_A to M becomes remarkable which could no longer be neglected. It could be concluded from Fig. 3(c) that the M-integral represents the level of the interaction effect and the coalescence tendency between the two collinear microcracks although it has been proved to be the summation of the two parts, i.e., M_N and M_A. The larger interaction effect between the two microcracks, the larger value of M in magnitude. Of course, when the interaction effect becomes smaller corresponding to the case that the two collinear microcracks are located far apart, the net-part of the M-integral, i.e., M_N, provides a good approximation to the M-integral. Moreover, it is seen in Fig. 3(a)–(c) that the imaginary curves (Cu/Al_2O_3) and the dotted curves (Ni/MgO) have significant divergencies from the real curves corresponding to homogeneous cases. Obviously, this is due to the mismatch nature of the bimaterial solids, Ni/MgO and Cu/Al_2O_3. It could be seen that the existence of the ductile phase, Cu or Ni, always leads to increase M_N and decrease M_A, and in turn to increase M. It is concluded that this kind of collinear microcrack arrangement in the brittle phase of the metal/ceramic bimaterial solids shows less stable nature and larger coalescence tendency than the corresponding one in homogeneous solids due to the existence of ductile phases and that the M-integral actually plays an important role to describe microcrack damage in bimaterial solids. Of great interest is the influence of the ductile phase on the above mentioned divergencies of M_N, M_A, and M which is obviously governed by the first Dundurs parameter α with no regards to the second parameter β. As shown in Table 1, $\alpha = -0.138$ for Ni/MgO and $\alpha = -0.5118$ for Cu/Al_2O_3 (see Hutchinson et al. 1987), while $\alpha = 0$ for homogeneous solids. This means that the value of α for Cu/Al_2O_3 shows larger deviation from zero (corresponding to homogeneous solids) than the value of α for Ni/MgO. Indeed, it is this reason that the computed values of M_N, M_A, and M for Cu/Al_2O_3 bimaterial show larger divergencies from the values for homogeneous solids than those for Ni/MgO bimaterial. Nevertheless to say, the second parameter β has no such a nature (see Table 1). In other words, it is the first parameter α rather than the second parameter β that dominates the divergencies of the imaginary curves and the dotted curves from the real curves in Fig. 3(a)–(c). Moreover, as the computed values of M for metal/ceramic bimaterial solids are always much larger than those for homogeneous solids, it is concluded that a certain microcrack array in the brittle phase of metal/ceramic bimaterial solids shows lower stability and larger coalescence tendency than the same microcrack array in homogeneous brittle solids.

Consider the microcrack arrangement shown in Fig. 2(b). Computed values of M_N, M_A, and M against the location angle α_0 with $d/a = 4.0$ and $h/a = 1.25$ are plotted in Fig. 4(a)–(c), respectively. It is seen that the similar conclusions could be given as those mentioned above for Fig. 2(a). Indeed, the values of M_N, M_A, and M for Cu/Al_2O_3 bimaterial (imaginary curves) and for Ni/MgO bimaterial (dotted curves) show large divergencies from those for homogeneous solids (real curves). These divergencies are also governed by the first Dundurs parameter α rather than β. It is also seen that, to a certain degree, for example, when the location angle α_0 is between 40° and 140°, the net part of the M-integral, i.e., M_N, overwhelming the additional part, i.e., M_A, becomes a good approximation of the M-integral with errors less than ten percent. However, when taking $\alpha_0 < 40°$ or $\alpha_0 > 140°$, especially when taking $\alpha_0 < 30°$ or $\alpha_0 > 150°$, the contribution of M_A to the M-integral could no longer be neglected. Of great interest is that the values of the M-integral in Fig. 4(c) for metal/ceramic bimaterial solids are always larger than the corresponding values for homogeneous brittle solids. This confirms again that a certain microcrack array in the brittle phase of metal/ceramics bimaterial solids shows lower stability and larger coalescence tendency than the same microcrack array in homogeneous brittle solids.

Consider the microcrack arrangement shown in Fig. 2(c). Computed values of M_N, M_A, and M against the oriented angle ϕ_0 with $h/a = 1.25$ and $d/a = 4.33$ are plotted in Fig. 5(a)–(c), respectively. Although the microcrack arrangement is quite different from the above discussed two examples, the similar conclusions could still be given. The values of M_N in metal/ceramic bimaterial solids are always larger than those derived in homogeneous solids. Quite contrary, the values of M_A in metal/ceramic bimaterial solids are

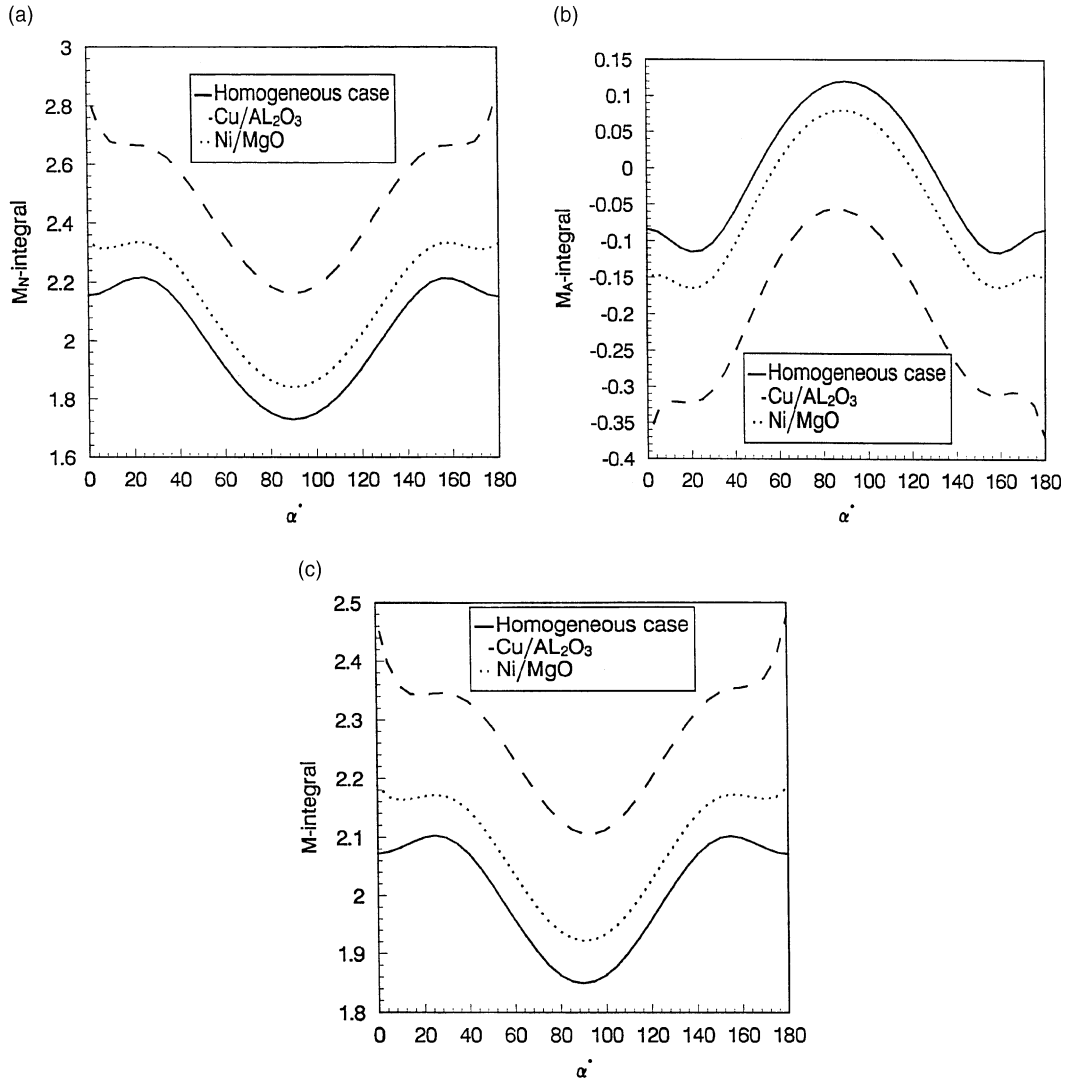

Fig. 4. (a)–(c) M_N, M_A, and M against α_0 for the case of Fig. 2(b).

always smaller than those derived in homogeneous solids. There exist apparently significant divergencies of the values of M in bimaterial solids from those in homogeneous brittle solids. The divergencies are actually governed by the first Dundurs parameter α with no regards to the second parameter β. What's more, the larger divergency of α from zero, the larger divergencies of M from those for homogeneous brittle solids.

Finally, consider the microcrack arrangement shown in Fig. 2(d). Computed values of M_N, M_A, and M against the oriented angle ϕ_0 with $h/a = 2.0$ and $d/a = 1.2$ are plotted in Fig. 6(a)–(c), respectively. Although the microcrack arrangement is quite different from the above discussed three examples, the similar conclusions could be given, which are no longer repeated here for shortening the length of this paper.

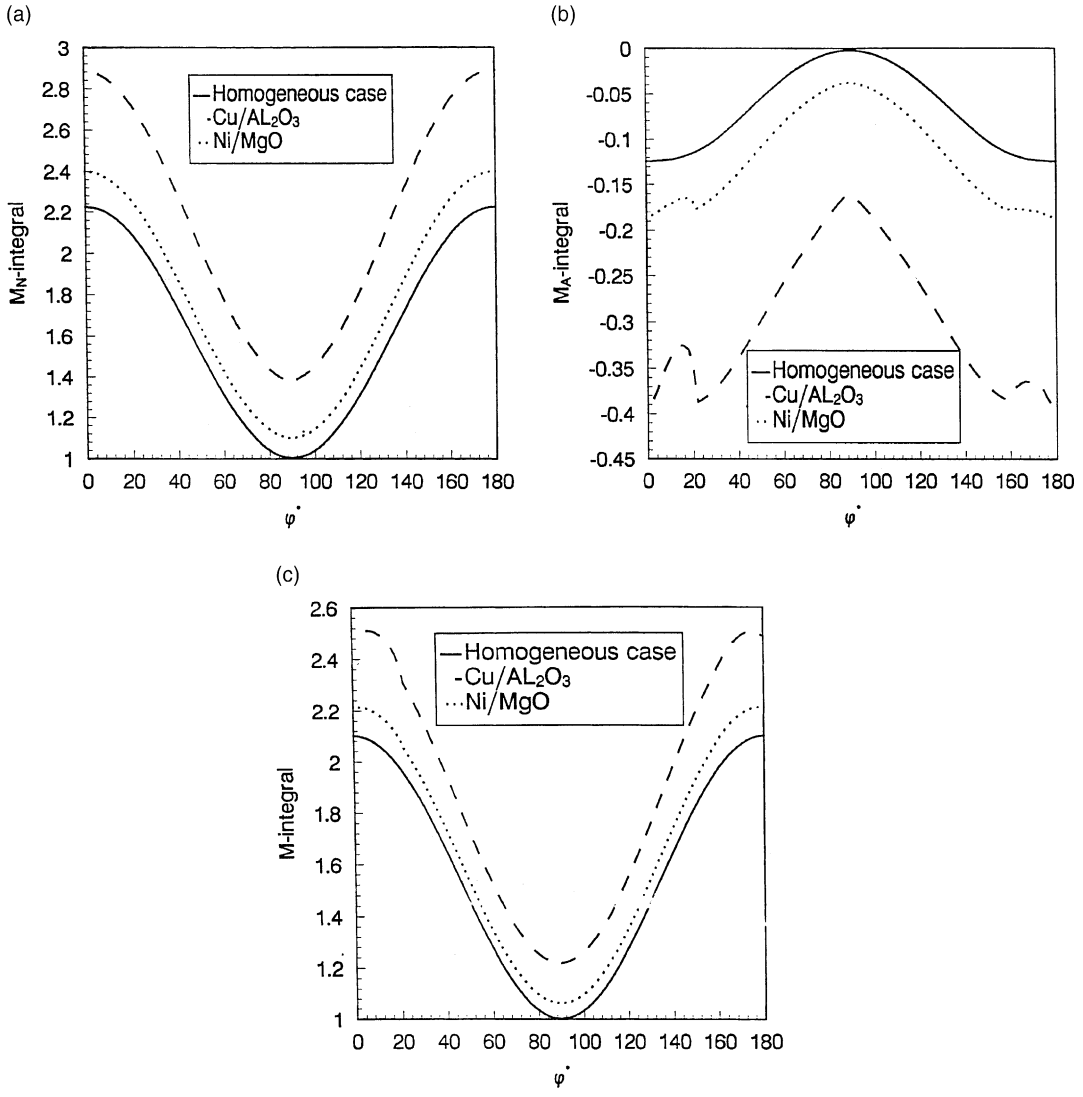

Fig. 5. (a)–(c) M_N, M_A, and M against φ_0 for the case of Fig. 2(c).

4.2. Four microcracks

Four interacting microcracks beneath the interface in the brittle phase of bimaterial solids are shown in Fig. 7. Take the lengths of the microcracks to be the same and take the normalized center-to-center distances to be equal with each other ($d/a = 2.25$). While the oriented angle ϕ_0 is taken to be a variable from 0° to 90° and the normalized distance between the interface and the neighbouring microcracks to be $h/a = 1.2$ (see Fig. 7).

Computed values of M_N, M_A, and M against the oriented angle ϕ_0 are plotted in Fig. 8(a)–(c), respectively. It is seen that the conclusions derived in two microcracks arrangements could still be given in the present case for the four microcracks arrangement. It is concluded that the conclusions given in this paper

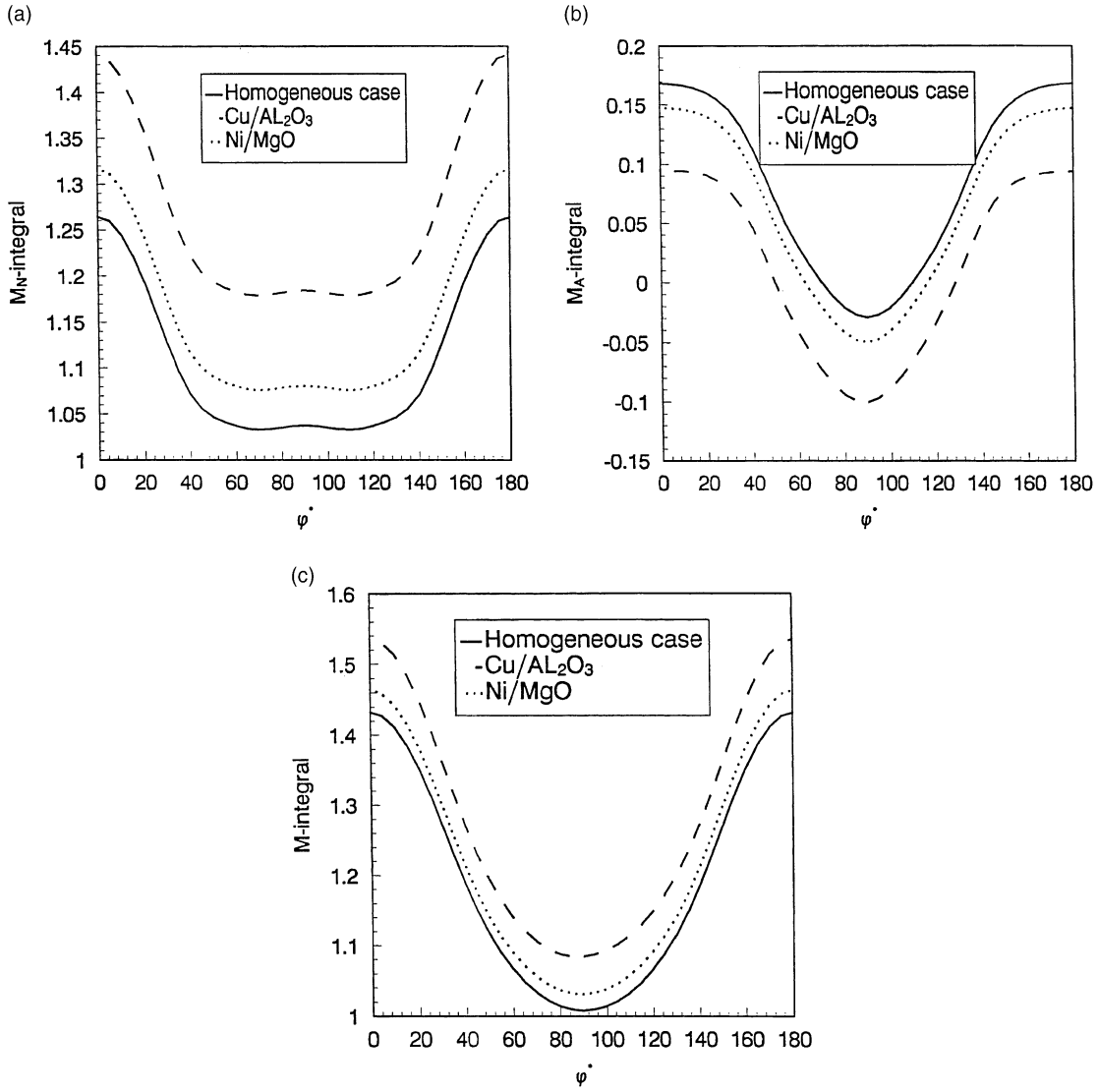

Fig. 6. (a)–(c) M_N, M_A, and M against φ_0 for the case of Fig. 2(d).

are inherent in the M-integral analysis no matter what kind of microcrack configurations in the brittle phase is considered, providing that the microcracks are stationary, fully open, and not intersected.

4.3. A half plane brittle solid containing multi-cracks

In order to show the potential applications of the present investigation, an extension of the present investigation to treat the multi-cracks problem in a half plane brittle solid is discussed briefly (see Fig. 9). Here, the outside boundary of the solid is taken along the x_1-axis, which is considered as a special kind of interface between air and the solid with the first Dundurs parameter $\alpha = -1$. The global coordinate system is originated at a fixed point on the boundary. The remote loading is preferred along the x_1-axis only. A

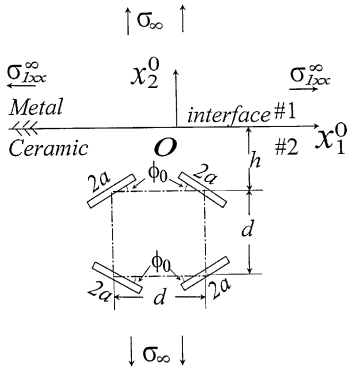

Fig. 7. Four microcracks beneath the interface.

two-crack array is considered. The left crack is taken as always perpendicular to the boundary, while the right crack is oriented by an angle ϕ_0, which is taken as a variable from 5° to 175°. The normalized distance $h/a = 1.25$ and $d/a = 1.25\sqrt{3}$. It is found that the M-integral takes the same variable tendencies for the three different kinds of material combinations (Air/Al_2O_3 with $\alpha = -1$, Cu/Al_2O_3 with $\alpha = -0.5118$, and Ni/MgO with $\alpha = -0.138$) (Fig. 10). However, there exist apparent divergencies among the three curves respectively corresponding to the real curve, the dotted curve, and the imaginary curve. As discussed above, the divergencies are dominated by the first Dundurs parameter α. The larger divergency of the parameter is from zero, the larger value of the M-integral is deduced. It is concluded that the outside boundary of the half plane solid could actually be treated as the special kind of interface between air and the brittle solid.

Therefore, the role the outside boundary plays in the M-integral analysis has been clarified. The present investigation could then easily be extended to treat a finite plane solid containing multi-cracks without any difficulties. The major idea is that the outside boundaries of the solid should be treated as a special kind of interface between air and the solid (or between a rigid body and the solid). Detailed manipulations and numerical examinations are beyond the scope of this paper.

5. Summary

From the above mentioned discussions, the following summary could be given:

(1) Although the existence of interface yields considerable trouble, the M-integral in a metal/ceramic bimaterial solid with strongly interacting microcracks in its brittle phase is still divided into two distinct parts. As in homogeneous cases, the first part is induced from the stress intensity factors at all microcrack tips although the existence of the interface disturbs the values of the SIF's significantly. Of great interest is that the second part is proved to be induced only from the global coordinates of each microcrack center and the J_k-vector of each crack with no regards to the contribution induced from the existence of the interface. This is due to the fact that the M-integral is independent from the selection of the origin of the global coordinate system when the closed integral contour is chosen to be infinite large, i.e., not only all the microcracks, but also the whole interface are enclosed in it. Therefore, the origin of the system could always be chosen on a certain point of the interface. Moreover, it is found that, generally speaking, the first part of the M-integral (i.e., the net part M_N) does not make overwhelming superiority over the second part (i.e., the additional part M_A) for a certain microcrack array in the brittle phase.

(2) The M-integral plays an important role for microcrack damage in the brittle phase of metal/ceramic bimaterial solids. It could be considered as a measure of the damage level, the microcrack stability, and the

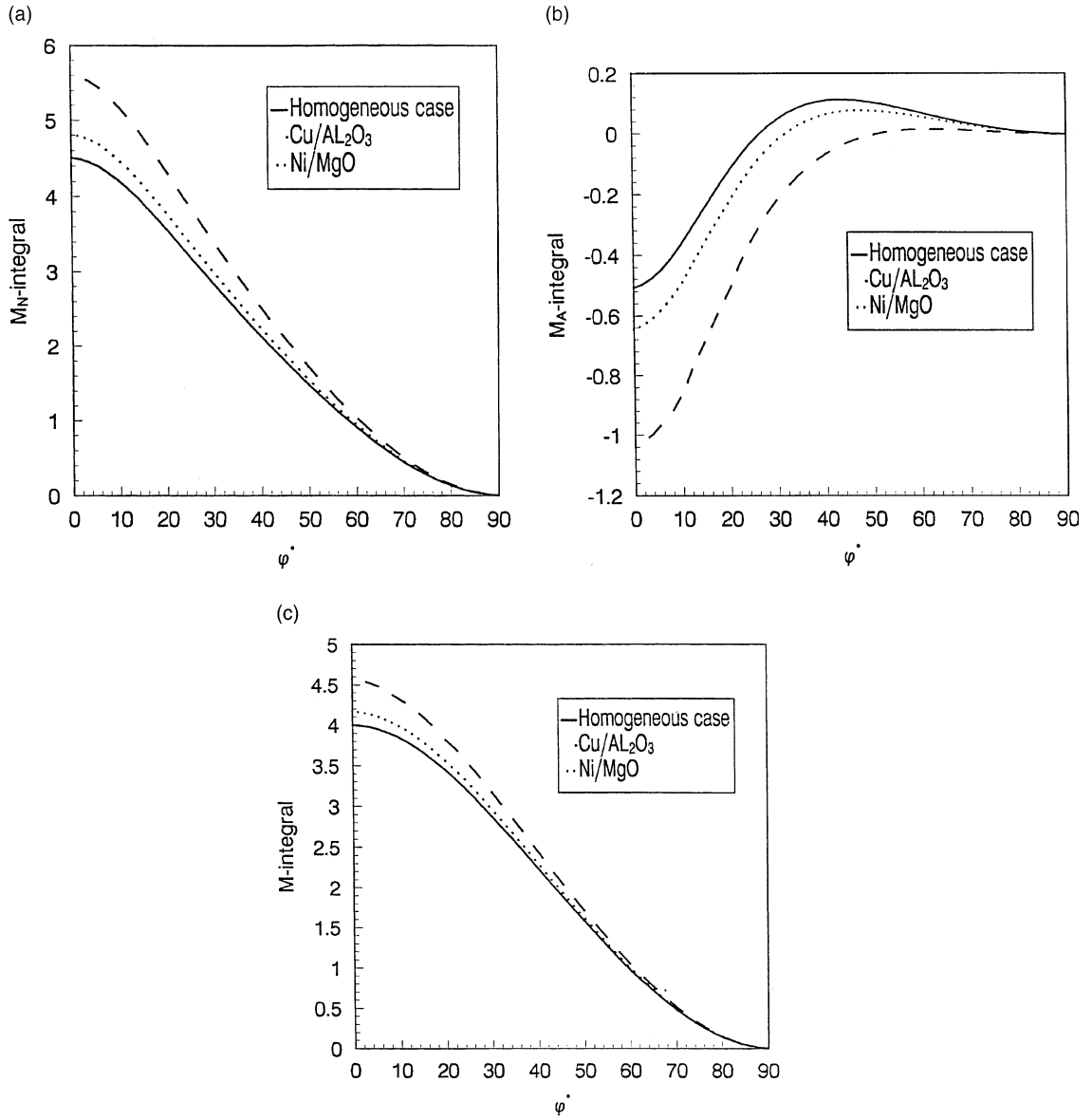

Fig. 8. (a)–(c) M_N, M_A, and M against φ_0 for the case of Fig. 7.

microcrack coalescence tendency. The present investigation does confirm the conclusions given in Part I of this series and does extend the M-integral analysis to treat multi-crack problems in much more complicated cases. It actually provides a new way to describe the microcrack damage phenomena, at least, in brittle solids, in the brittle phase of metal/ceramic bimaterial solids, and in half plane brittle solids. It is found that the restriction arising from the investigation in Part I, i.e., the manipulations are only valid in an infinite case, could be removed without doubt.

(3) There always exist significant divergencies of the M-integral values in metal/ceramic bimaterial solids from those for the same microcrack array in homogeneous brittle solids. The divergencies are governed by

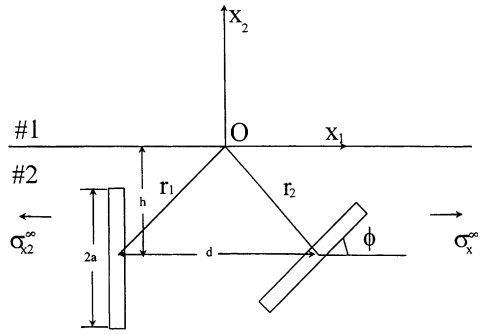

Fig. 9. A half plane brittle solid containing multi-cracks.

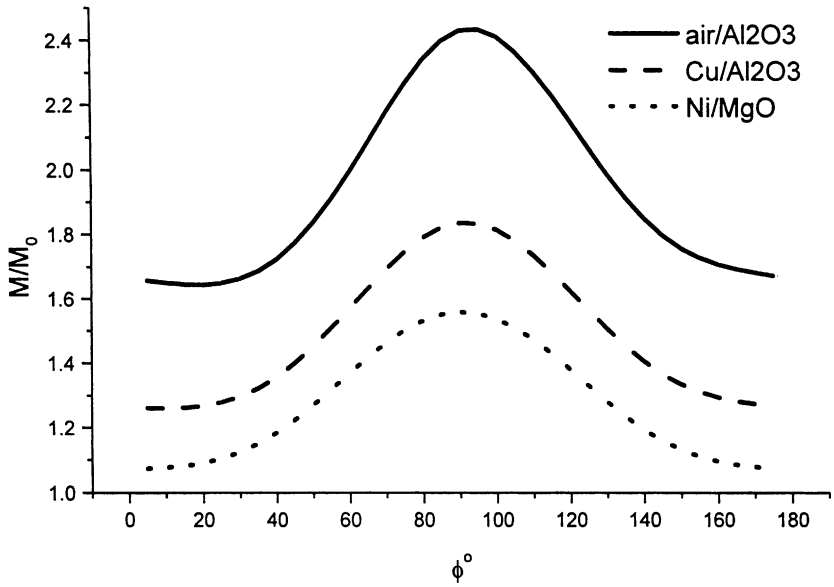

Fig. 10. Variable tendencies of the M-integral for three kinds of material combinations.

the first Dundurs parameter α with no regards to the second parameter β. The larger divergency of α from zero, the larger divergencies of the values of the M-integral in metal/ceramic solids from those in homogeneous brittle solids, providing that the same microcrack configuration is considered in both kinds of solids.

(4) For the same kind of microcrack array, the values of the M-integral in the brittle phase of a metal/ceramic bimaterial are always larger than those in a homogeneous brittle solid. This is due to the existence of the ductile phase or due to the interaction of the microcrack array with the interface. Therefore, it is concluded that a certain microcrack array in the former case shows lower stability and larger coalescence tendency than the same array in the later case. Of course, the largest value of the M-integral occurs for the same microcrack array in air/brittle bimaterial since the first Dundurs parameter takes -1 corresponding to the largest divergence from zero (homogeneous cases).

(5) The brief investigation for a half plane brittle solid shows that the M-integral analysis could be extended to treat microcrack damage problems in a finite brittle solid. The only correct way is to consider the outside boundaries of the finite solid as a special kind of interface between air and the solid (or between a rigid body and the solid). This topic will be discussed in detail in the present author's sequential papers.

Acknowledgements

This work was supported by the Chinese National Natural Science Foundation and by the *DAAD* foundation of Germany.

References

Budiansky, B., Rice, J.R., 1973. Conservation laws and energy-release rates. ASME J. Appl. Mech. 40, 201–203.
Chen, B., Lardner, T.J., 1993. Two-dimensional cracks at an angle to an interface. Int. J. Solids Struct. 30, 1725–1735.
Chen, Y.Z., 1985. New path independent integrals in linear elastic fracture mechanics. Engng. Fract. Mech. 22, 673–686.
Chen, Y.Z., Hasebe, N., 1994. Eigen function expansion and higher order weight functions of interface cracks. ASME J. Appl. Mech. 61, 843–849.
Evans, A.G., Lu, M.C., Schmander, S., Ruhle, M., 1986. Some aspects of the mechanical strength of ceramic/metal bonded systems. Acta Metall. Mater. 34, 1643–1655.
Freund, L.B., 1978. Stress intensity factor calculation based on a conservation integral. Int. J. Solids Struct. 14, 241–250.
Herrmann, A.G., Herrmann, G., 1981. On energy release rates for a plane crack. ASME J. Appl. Mech. 48, 525–530.
He, M.Y., Hutchinson, J.W., 1989. Crack deflection at an interface between dissimilar elastic materials. Int. J. Solids Struct. 25, 1053–1067.
Hutchinson, J.W., Mear, M.E., Rice, J.R., 1987. Crack paralleling an interface between dissimilar materials. ASME J. Appl. Mech. 54, 828–832.
Isida, M., Noguchi, H., 1994. Distributed cracks and kinked cracks in bonded dissimilar planes with an interface. Int. J. Fract. 66, 313–337.
Knowles, J.K., Sternberg, E., 1972. On a class of conservation laws in lineared and finite elastostatics. Arch. Rat. Mech. Anal. 44, 187–211.
Lardner, T.J., Ritter, J.E., Shiao, M.L., Lin, M.R., 1990. Behavior of indentation cracks near free surfaces and interfaces. Int. J. Fract. 44, 133–143.
Lu, H., Lardner, T.J., 1992. Mechanics of subinterface cracks in layered materials. Int. J. Solids Struct. 29, 669–688.
Park, J.H., Earmme, Y.Y., 1986. Application of conservation integrals to interface crack problems. Mech. Mater. 5, 261–276.
Rice, J.R., 1968. A path independent integral and the approximate analysis of strain conservation by notches and cracks. ASME J. Appl. Mech. 35, 379–386.
Rice, J.R., 1988. Elastic fracture mechanics concept for interfacial cracks. ASME J. Appl. Mech. 55, 98–103.
Smelser, R.E., Gurtin, E., 1977. On the J-integral for bi-material bodies. Int. J. Fract. 13, 382–384.
Stern, M., Becker, E.B., Dunham, R.S., 1976. A contour integral computation of mixed-mode stress intensity factors. Int. J. Fract. 12, 359–368.
Suo, Z., Hutchinson, J.W., 1989. Steady-state cracking in brittle substrates beneath adherent films. Int. J. Solids Struct. 25, 1337–1353.
Suo, Z., 1989. Singularities interacting with interface and cracks. Int. J. Solids Struct. 25, 1133–1142.
Suo, Z., Hutchinson, J.W., 1990. Interface crack between two elastic layers. Int. J. Fract. 43, 1–18.
Zhao, L.G., Chen, Y.H., 1996. Interaction between an interface crack and a parallel subinterface crack. Int. J. Fract. 76, 279–291.
Zhao, L.G., Chen, Y.H., 1997a. On the contribution of subinterface microcracks near the tip of an interface crack to the J-integral in bimaterial solids. Int. J. Engng. Sci. 35, 387–407.
Zhao, L.G., Chen, Y.H., 1997b. Further investigation of subinterface cracks. Arch. of Appl. Mech. 67, 393–406.